

Molecular Hypergraph Grammar with Its Application to Molecular Optimization

Hiroshi Kajino
kajino@jp.ibm.com¹

¹MIT-IBM Watson AI Lab, IBM Research

August 9, 2022

Abstract

This paper is concerned with a molecular optimization framework using variational autoencoders (VAEs). In this paradigm, VAE allows us to convert a molecular graph into/from its latent continuous vector, and therefore, the molecular optimization problem can be solved by continuous optimization techniques. One of the longstanding issues in this area is that it is difficult to always generate valid molecules. The very recent work called the junction tree variational autoencoder (JT-VAE) successfully solved this issue by generating a molecule fragment-by-fragment. While it achieves the state-of-the-art performance, it requires several neural networks to be trained, which predict which atoms are used to connect fragments and stereochemistry of each bond. In this paper, we present a molecular hypergraph grammar variational autoencoder (MHG-VAE), which uses a single VAE to address the issue. Our idea is to develop a novel graph grammar for molecular graphs called *molecular hypergraph grammar* (MHG), which can specify the connections between fragments and the stereochemistry on behalf of neural networks. This capability allows us to address the issue using only a single VAE. We empirically demonstrate the effectiveness of MHG-VAE over existing methods.

1 Introduction

Molecular optimization aims to discover a novel molecule that possesses prescribed properties given by a user. For example, Gómez-Bombarelli et al. (2016) aim to maximize the efficiency of an organic light-emitting diode. Letting \mathcal{M} be a set of valid molecules, the molecular optimization problem is to obtain $m^* \in \mathcal{M}$ such that,

$$m^* = \arg \max_{m \in \mathcal{M}} f(m), \quad (1)$$

where $f: \mathcal{M} \rightarrow \mathbb{R}$ is an unknown function that outputs a chemical property of the input molecule to be maximized.

There are two obstacles to solve Problem 1. First, f is unknown and costly to evaluate, and only finite examples $\{(m_1, y_1), \dots, (m_N, y_N)\} \subset \mathcal{M} \times \mathbb{R}$ are available in reality. Second, the set of feasible solutions \mathcal{M} is discrete, and it is difficult to generate a candidate m from \mathcal{M} .

A recent innovation (Gómez-Bombarelli et al., 2018)¹ significantly facilitates the optimization by leveraging a variational autoencoder (VAE) (Kingma and Welling, 2014). The first challenge is addressed by using a Bayesian optimization (BO) technique (Moćkus, 1975), which allows us to optimize a black-box function. The second one is addressed by casting the discrete optimization problem to a continuous one with the help of VAE. In specific, they first train an autoencoder², a pair of $\text{Enc}: \mathcal{M} \rightarrow \mathbb{R}^D$ and $\text{Dec}: \mathbb{R}^D \rightarrow \mathcal{M}$ such that $\text{Dec}(\text{Enc}(m)) \approx m$ holds for any $m \in \mathcal{M}$, and they obtain m^* as follows:

$$m^* = \text{Dec} \left(\arg \max_{z \in \mathbb{R}^D} f(\text{Dec}(z)) \right), \quad (2)$$

where the inner optimization problem is solved by BO with sample $\{(\text{Enc}(m_1), y_1), \dots, (\text{Enc}(m_N), y_N)\} \subset \mathbb{R}^D \times \mathbb{R}$.

¹Its arXiv preprint appeared in 2016.

²Note that the encoder of VAE outputs a random variable.

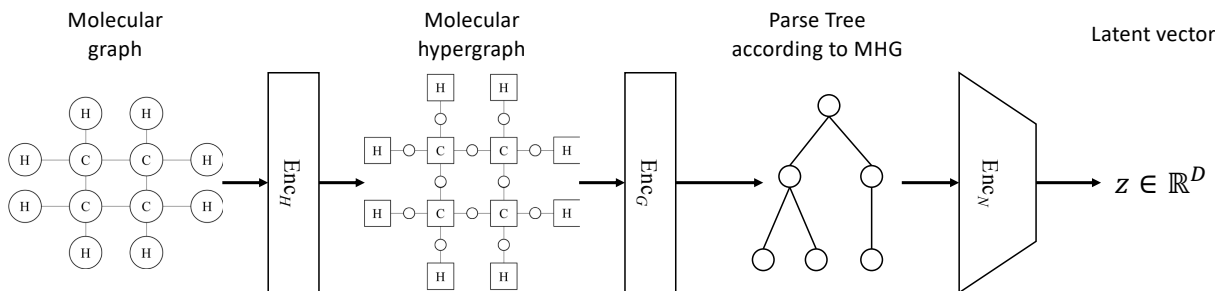


Figure 1: Illustration of our encoder. For a molecular hypergraph, squares represent hyperedges, circles represent nodes, and a circle-square line indicates that the node is a member of the hyperedge. The decoder is defined by inverting the encoder.

While they elegantly address the two obstacles, the decoding sometimes fails, and no molecule is obtained, which we call the *decoding error issue*. Let us explain this issue in detail. They use a string representation of a molecule called SMILES (Weininger, 1988) as the intermediate representation. Let Σ be a set of symbols used in SMILES, and $\text{Enc}_S: \mathcal{M} \rightarrow \Sigma^*$ be a SMILES encoder. For example, Σ includes atomic symbols, e.g., $\text{C}, \text{H} \in \Sigma$; given a phenol as input, the encoder outputs c1c(O)cccc1, where the digits represent the start and end points of the benzene ring, the parentheses represent branching, and hydrogen atoms are omitted. Letting $\text{Enc}_S[\mathcal{M}] := \{\text{Enc}_S(m) \mid m \in \mathcal{M}\} \subsetneq \Sigma^*$ be the set of all *valid* SMILES strings, a SMILES decoder $\text{Dec}_S: \text{Enc}_S[\mathcal{M}] \rightarrow \mathcal{M}$ can be defined; the domain of the decoder cannot be Σ^* but the set of strings that follow SMILES’ grammar, $\text{Enc}_S[\mathcal{M}]$, because any string that violates the grammar cannot be decoded into any molecule. In their implementation, the encoder is composed as $\text{Enc} = \text{Enc}_N \circ \text{Enc}_S$, where $\text{Enc}_N: \Sigma^* \rightarrow \mathbb{R}^D$ is a neural network encoder, and the decoder is composed as $\text{Dec} = \text{Dec}_S \circ \text{Dec}_N$, where $\text{Dec}_N: \mathbb{R}^D \rightarrow \Sigma^*$ is a neural network decoder, generating symbols one by one.

The decoding error issue occurs when the output of Dec_N does not belong to $\text{Enc}_S[\mathcal{M}]$, the domain of Dec_S . For the phenol example, if Dec_N fails to output the end digit, e.g., c1c(O)cccc, the output string cannot be converted into a molecule because the ring cannot be closed. For another example, if Dec_N generates more than one pair of parentheses, e.g., c1c(O)(O)cccc1, the output string violates the valence condition of carbon. Since SMILES’ grammar is a context-sensitive grammar, it is not straightforward to develop a neural network that is guaranteed to generate a string that belongs to $\text{Enc}_S[\mathcal{M}]$.

Recently, several studies have been conducted towards addressing the decoding error issue (Kusner et al., 2017; Dai et al., 2018; Jin et al., 2018). Among them, Jin et al. (2018) for the first time report 100% validity, addressing the decoding error issue. The key idea is to represent a molecular graph by fragments (such as rings and atom branches) connected in a tree structure. Such a tree representation is preferable because it is easier to generate a tree than a general graph with degree constraints. By forcing the decoder to generate only valid combination of fragments, the decoder can always generate a valid molecule.

While their tree representation successfully addresses the decoding error issue, it models only part of molecular properties, and the rest is left to neural networks. For example, their representation only specifies fragment-level connections, and does not specify which atoms in the fragments to be connected. In addition, since it does not specify atom-level connections, the stereochemistry information disappears. They instead enumerate all possible configurations and pick one by training several additional neural networks.

Our idea to address the decoding error issue without relying on multiple neural networks is to develop a (i) *context-free* graph grammar of a molecular graph that (ii) *never generates an invalid molecule*, and that (iii) *can represent the atom-level connection and stereochemistry information*. With such a grammar, we can use a parse tree as a tree representation of a molecule. The context-freeness (i) allows us to easily force the decoder of VAE to generate a valid parse tree. Combined with the properties (ii) and (iii), our decoder can always output a valid molecule with stereochemistry information, using a single VAE only.

We develop a *molecular hypergraph grammar* (MHG), which satisfies all of the requirements mentioned above, along with an algorithm to infer MHG from a set of molecules. We also develop a molecular hypergraph grammar variational autoencoder (MHG-VAE), which combines MHG and VAE to obtain an autoencoder for a molecule. Figure 1 illustrates our encoder, where the first two encoders, Enc_H and Enc_G , and their corresponding decoders Dec_H and Dec_G , are our main contributions, while we use a standard seq2seq VAE as $(\text{Enc}_N, \text{Dec}_N)$.

In specific, we develop MHG by applying a hyperedge replacement grammar (HRG) (Drewes et al., 1997) to a molecular hypergraph (thus, MHG is a special case of HRG). A molecular hypergraph models an atom by a hyperedge and a bond by a node. HRG is a context-free graph grammar generating a hypergraph by replacing a hyperedge with another hypergraph; it achieves atom-level connections when combined with a molecular hypergraph, and stereochemistry can also be encoded into

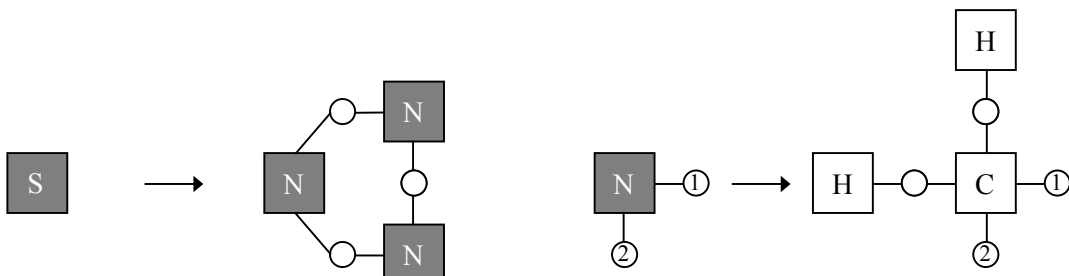


Figure 2: Part of production rules extracted from the hypergraph in Figure 1. Filled squares represent non-terminals, and unfilled ones represent terminals. Numbers in nodes indicate the correspondence between the nodes in A and R .

the grammar. A key property of HRG is that it preserves the number of nodes belonging to each hyperedge, which coincides with the valency of an atom in the case of a molecular hypergraph. Therefore, these two ideas allow us to always generate valid molecules using a single VAE.

Our MHG inference algorithm extends the existing HRG inference algorithm (Aguinaga et al., 2016) so that the resultant HRG always generates a molecular hypergraph. The existing one infers HRG by extracting a set of production rules from a tree decomposition of each hypergraph, which is equivalent to a parse tree. Our finding is that, while the inferred HRG preserves the valence condition, it can generate a hypergraph that cannot be decoded into a molecular graph; the generated hypergraph may contain a node that is shared by more than two hyperedges. To address this issue, we develop an *irredundant* tree decomposition, with which HRG is guaranteed to generate a valid molecular hypergraph, *i.e.*, the inferred HRG is MHG.

2 Preliminaries

First of all, we briefly introduce three fundamental notions, a hypergraph, a tree decomposition of a hypergraph, and a hyperedge replacement grammar (HRG).

A hypergraph is a pair $H = (V_H, E_H)$, where V_H is a set of nodes, and E_H is a set of non-empty subsets of V_H , called hyperedges. A hypergraph is called k -regular if every node has degree k .

A tree decomposition of a hypergraph (Definition 1) discovers a tree-like structure of the hypergraph. Figure 3 illustrates a tree decomposition of the hypergraph shown in Figure 1.

Definition 1. A tree decomposition of hypergraph $H = (V_H, E_H)$ is tree $T = (V_T, E_T)$ with two labeling functions $\ell_T^{(V)}: V_T \rightarrow 2^{V_H}$ and $\ell_T^{(E)}: V_T \rightarrow 2^{E_H}$ such that:

1. For each $v_H \in V_H$, there exists at least one node $v_T \in V_T$ such that $v_H \in \ell_T^{(V)}(v_T)$.
2. For each $e_H \in E_H$, there exists exactly one node $v_T \in V_T$ such that $e_H \subseteq \ell_T^{(V)}(v_T)$ and $e_H \in \ell_T^{(E)}(v_T)$.
3. For each $v_H \in V_H$, a set of nodes $\{v_T \in V_T \mid v_H \in \ell_T^{(V)}(v_T)\}$ is connected in T .

Let us denote the hypergraph on node $v_T \in V_T$ by $H(v_T) := (\ell_T^{(V)}(v_T), \ell_T^{(E)}(v_T))$.

HRG (Drewes et al., 1997) is a context-free grammar generating hypergraphs with labeled nodes³ and hyperedges (Definition 2, Figure 2). It starts from the starting symbol S and repeatedly replaces a non-terminal symbol A in the hypergraph with a hypergraph R , which may have both terminal and non-terminal symbols.

Definition 2. A hyperedge replacement grammar is a tuple $\text{HRG} = (N, T, S, P)$, where,

1. N is a set of non-terminal hyperedge labels.
2. T is a set of terminal hyperedge labels.
3. $S \in N$ is a starting non-terminal hyperedge.

³Node labels are handled by encoding them in hyperedge labels.

4. P is a set of production rules where,

- $p = (A, R)$ is a production rule,
- $A \in N$ is a non-terminal symbol, and
- R is a hypergraph with hyperedge labels $T \cup N$ and has $|A|$ external nodes. Non-terminals in R are ordered.

We define a *parse tree* according to HRG as follows. Each node of the parse tree is labeled by a production rule. The production rules of the leaves of the parse tree must not contain non-terminals in their R s. If the production rule p is a starting rule, the node has N_p ordered children, where N_p denotes the number of non-terminals in R , and the edges are ordered by the orders of the non-terminals. Otherwise, the node has one parent and N_p ordered children, where the corresponding non-terminal in the parental production rule must coincide with A of the production rule.

Given a parse tree, we can construct a hypergraph by sequentially applying the production rules. Such sequential applications of production rules are equivalent to the parse tree, and we call it a *parse sequence*.

3 Molecular Graph and Hypergraph

This section introduces the definitions of a molecular graph and a molecular hypergraph. We also present a pair of encoder and decoder between them, $(\text{Enc}_H, \text{Dec}_H)$.

3.1 Molecular Graph

A molecular graph (Definition 3) represents the structural formula of a molecule using a graph, where atoms are modeled as labeled nodes and bonds as labeled edges. Typically, the node label is defined by the atom’s symbol (e.g., H, C) and its formal charge, and the edge label by the bond type (e.g., single, double). The graph must satisfy the valency condition; the degree of each atom is specified by its label (e.g., the degree of C must equal four). Let $\mathcal{G}(L_G^{(V)}, L_G^{(E)}, d^{(V)})$ be the set of all possible molecular graphs, given the sets of node and edge labels and the degree constraint function.

Definition 3. Let $L_G^{(V)}$ and $L_G^{(E)}$ be sets of node and edge labels. Let $d^{(V)}: L_G^{(V)} \rightarrow \mathbb{N}$ be a degree constraint function. Let $G = (V_G, E_G, \ell_G^{(V)}, \ell_G^{(E)})$ be a node and edge-labeled graph, where V_G is a set of nodes, E_G is a set of undirected edges, $\ell_G^{(V)}: V_G \rightarrow L_G^{(V)}$ is a node-labeling function, and $\ell_G^{(E)}: E_G \rightarrow L_G^{(E)}$ is an edge-labeling function. A molecular graph G is a node and edge-labeled graph that satisfies $d(v) = d^{(V)}(\ell_G^{(V)}(v))$ for all $v \in V_G$, where $d(v)$ indicates the degree of node v .

There are two types of important properties that influence the chemical properties of a molecule. The first one is the aromaticity of a ring (e.g., benzene derivatives). The bonds in an aromatic ring are different from a single or double bond, and are known to be more stable. We do not explicitly encode any information related to the aromaticity, and instead, employ the Kekul structure, where an aromatic ring is represented by alternating single and double bonds. This does not lose generality because we can infer the aromaticity from the Kekul representation.

The second one is the stereochemistry, which specifies 2D or 3D configuration of atoms. We deal with the configuration at a double bond and tetrahedral carbon. The double bond configuration is encoded by an E-Z configuration label assigned on the edge label. Given the label and the whole structure of the molecule, the CahnIngoldPrelog priority rules can specify the double bond direction. For the tetrahedral chirality information, we assign a chirality tag in the node label, following the implementation of RDKit.

In summary, we employ the graph representation (Definition 3), where the node label contains the atom symbol, formal charge, and the tetrahedral chirality tag, and the edge label contains the bond type and the E-Z configuration.

3.2 Molecular Hypergraph

As an intermediate representation, we use a molecular hypergraph (Definition 4), where an atom is modeled by a hyperedge and a bond between two atoms by a node shared by the corresponding two hyperedges. Let $\mathcal{H}(L_H^{(V)}, L_H^{(E)}, c^{(E)})$ be the set of all molecular hypergraphs, given the sets of node and hyperedge labels and the cardinality constraint function.

Definition 4. Let $L_H^{(E)}$ and $L_H^{(V)}$ be sets of hyperedge and node labels. Let $c^{(E)}: L_H^{(E)} \rightarrow \mathbb{N}$ be a cardinality constraint function. Let $H = (V_H, E_H, \ell_H^{(E)}, \ell_H^{(V)})$ be a node and hyperedge-labeled hypergraph, where V_H is a set of nodes, E_H is a

set of hyperedges, $\ell_H^{(V)}: V_H \rightarrow L_H^{(V)}$ is a node-labeling function, and $\ell_H^{(E)}: E_H \rightarrow L_H^{(E)}$ is a hyperedge-labeling function. A molecular hypergraph H is a node and hyperedge-labeled hypergraph that satisfies the followings:

1. (Regularity) H is 2-regular.
2. (Cardinality) for each $e \in E_H$, $|e| = c^{(E)}(\ell_H^{(E)}(e))$ holds, where $|e|$ is the cardinality of hyperedge e .

Note that the regularity condition in Definition 4 assures that any molecular hypergraph can be decoded into a graph.

3.3 Encoder and Decoder between Molecular Graph and Hypergraph

Finally, we present the encoder and decoder between a molecular graph and a molecular hypergraph, $(\text{Enc}_H, \text{Dec}_H)$. They can be derived easily by swapping nodes-hyperedges and edges-nodes. The regularity condition assures the swap to work. This equivalence immediately yields the following:

Theorem 1. If $L_G^{(V)} = L_H^{(E)}$, $L_G^{(E)} = L_H^{(V)}$, and $d^{(V)}(l) = c^{(E)}(l)$ for all $l \in L_G^{(V)}$ hold, then the followings hold:

$$\begin{aligned}\mathcal{H}(L_H^{(V)}, L_H^{(E)}, c^{(E)}) &= \text{Enc}_H[\mathcal{G}(L_G^{(V)}, L_G^{(E)}, d^{(V)})], \\ \mathcal{G}(L_G^{(V)}, L_G^{(E)}, d^{(V)}) &= \text{Dec}_H[\mathcal{H}(L_H^{(V)}, L_H^{(E)}, c^{(E)})], \\ G = \text{Dec}_H(\text{Enc}_H(G)) &(\forall G \in \mathcal{G}(L_G^{(V)}, L_G^{(E)}, d^{(V)})).\end{aligned}$$

4 Molecular Hypergraph Grammar

A molecular hypergraph grammar (MHG) is defined as an HRG that always generates molecular hypergraphs. In this section, we present $(\text{Enc}_G, \text{Dec}_G)$ that leverages MHG to represent a molecular hypergraph as a parse sequence.

Let $\text{MHG} = (N, T, S, P)$ be a molecular hypergraph grammar, and \mathcal{L}_{MHG} be its language, *i.e.*, the set of molecular hypergraphs that can be generated by MHG. The encoder $\text{Enc}_G: \mathcal{L}_{\text{MHG}} \rightarrow P^*$ maps a molecular hypergraph into the corresponding parse sequence. The decoder maps a parse sequence into a molecular hypergraph by sequentially applying the production rules. It accepts a sequence of production rules obtained from \mathcal{L}_{MHG} only, because other sequences cannot generate a molecular hypergraph. Thus, the domain of the decoder is defined as $\text{Dec}_G: \text{Enc}_G[\mathcal{L}_{\text{MHG}}] \rightarrow \mathcal{L}_{\text{MHG}}$. Clearly, for any $H \in \mathcal{L}_{\text{MHG}}$, $H = \text{Dec}_G(\text{Enc}_G(H))$ holds.

5 MHG Inference Algorithm

We present an algorithm to infer MHG from a set of molecular hypergraphs. Our algorithm extends an existing HRG inference algorithm (Aguiñaga et al., 2016), which extracts a set of production rules from tree decompositions of hypergraphs. We observe that HRG inferred from molecular hypergraphs does not necessarily generate a molecular hypergraph; it sometimes violates the regularity condition (see the first condition in Definition 4). To this end, we develop a novel inference algorithm that preserves the regularity condition.

We first review the existing HRG inference algorithm (Section 5.1). Then, we present our MHG inference algorithm as well as its key component called an *irredundant* tree decomposition (Section 5.2). We also provide theoretical properties of our inference algorithm.

5.1 Existing HRG Inference Algorithm

Aguiñaga et al. (2016) propose an algorithm to infer HRG from a set of hypergraphs. Their key observation is that tree decompositions of hypergraphs yield HRG whose associated language includes the whole input hypergraphs.

Assume that we have a tree decomposition T of hypergraph H . We arbitrarily choose one node from T as the root node. For node $v_T \in V_T$, let $\text{pa}(v_T)$ be the parent of v_T and $\text{ch}(v_T)$ be a set of children of v_T . They first notice that connecting each pair $(v_T, \text{pa}(v_T))$ by their common nodes yields the original hypergraph (*e.g.*, connecting such pairs in Figure 3 yields the hypergraph in Figure 1). In other words, a tree decomposition with an arbitrary root node is equivalent to a parse tree. Given this observation, their algorithm extracts a production rule from a triplet $(\text{pa}(v_T), v_T, \text{ch}(v_T))$ so that the production rule can paste $H(v_T)$ on $H(\text{pa}(v_T))$ with non-terminals left for applying the following production rules obtained from the children. Note that the algorithm outputs not only HRG but also parse sequences of input hypergraphs. For more details, see Appendix A.

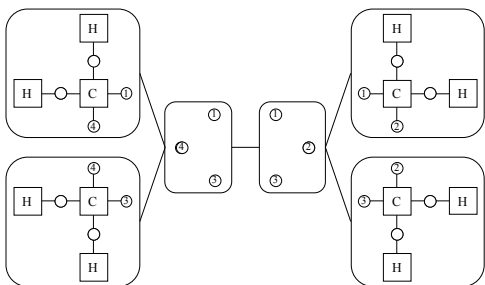


Figure 3: Irredundant tree decomposition of the hypergraph in Figure 1.

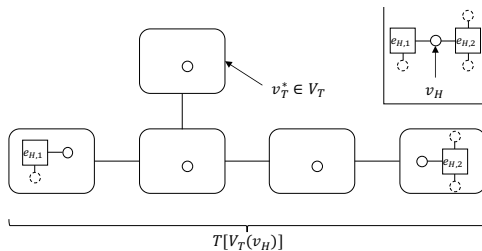


Figure 4: *Redundant* tree decomposition T . The upper-right shows a subhypergraph of H , whose tree decomposition induced by $V_T(v_H)$ is shown in the lower-left. It is necessary to remove v_H from v_T^* to transform it to be irredundant.

5.2 Our MHG Inference Algorithm

We find that the existing algorithm cannot infer MHG, *i.e.*, the inferred HRG sometimes violates the regularity condition. We develop an *irredundant* tree decomposition so that the violation does not occur, and substitute it for a generic tree decomposition to derive our MHG inference algorithm.

Irredundant Tree Decomposition. We introduce a key property of a tree decomposition called *irredundancy*, which is necessary to guarantee the regularity. Intuitively, a tree decomposition is irredundant if each node of the tree does not contain redundant nodes of the original hypergraph. Figures 3 and 4 illustrate both irredundant and redundant tree decompositions. The formal definition appears in Definition 5.

Definition 5. Let $H = (V_H, E_H)$ be a hypergraph, and $(T, \ell_T^{(V)}, \ell_T^{(E)})$ be its tree decomposition. Let $V_T(v_H) = \{v_T \in V_T \mid v_H \in \ell_T^{(V)}(v_T)\}$ be a set of nodes in T that contain $v_H \in V_H$. A tree decomposition is irredundant if,

$$\begin{aligned} \forall v_H \in V_H, \forall v_T \in V_T(v_H) \\ \ell_T^{(E)}(v_T) \neq \emptyset \Leftrightarrow v_T \text{ is a leaf in } T[V_T(v_H)], \end{aligned} \quad (3)$$

where $T[V_T(v_H)]$ is the subgraph induced by $V_T(v_H)$.

We can make any tree decomposition to be irredundant in polynomial time; for each v_H , if it does not satisfy the condition (3), remove v_H from each $\ell_T^{(E)}(v_T)$ ($v_T \in V_T(v_H)$).

Implementation. We tailor a tree decomposition algorithm for a molecular hypergraph. It starts from a one-node tree whose node contains the input hypergraph, and updates the tree by applying the following two steps.

The first step is to find a node such that the input hypergraph becomes disjoint when divided at the node, and to divide the hypergraph into two. When dividing a hypergraph at a node, the node is duplicated so that the two hyperedges that the node belonged to still contain the node. This operation is repeatedly applied to the subhypergraphs until there does not exist such a node. As a result, the input hypergraph is divided into (i) hypergraphs containing exactly one hyperedge and (ii) hypergraphs that contain rings. The type-(i) hypergraphs are obtained from tree structures of the input hypergraph, and the type-(ii) ones from ring structures.

The second step rips off the hyperedges from the type-(ii) hypergraphs. This operation is helpful to reduce the number of production rules; otherwise, since the number of possible atom configurations of a ring is enormous, that of production rules also greatly increases.

Theoretical Result. Theorem 2 summarizes the properties of our algorithm. It suggests that (i) HRG inferred by our algorithm can generate the whole input hypergraphs and (ii) the inferred HRG always generates a molecular hypergraph, *i.e.*, the HRG is MHG. For its proof, see Appendix B.

Theorem 2. Let $\mathcal{H}(L_H^{(V)}, L_H^{(E)}, c^{(E)})$ be a set of all molecular hypergraphs and $\hat{\mathcal{H}}$ be its finite subset. Let $\mathcal{L}_{\text{HRG}}(\hat{\mathcal{H}})$ be the language generated by HRG inferred by applying our algorithm to $\hat{\mathcal{H}}$. Then, $\mathcal{L}_{\text{HRG}}(\hat{\mathcal{H}})$ satisfies

$$\hat{\mathcal{H}} \subseteq \mathcal{L}_{\text{HRG}}(\hat{\mathcal{H}}) \subseteq \mathcal{H}(L_H^{(V)}, L_H^{(E)}, c^{(E)}).$$

6 Application to Molecular Optimization

So far, we have presented $(\text{Enc}_H, \text{Dec}_H)$, a pair of encoder and decoder between a molecular graph and a molecular hypergraph (Section 3.3), and $(\text{Enc}_G, \text{Dec}_G)$, that between a molecular hypergraph and a parse sequence according to MHG (Section 4). We have also provided an algorithm to obtain $(\text{Enc}_G, \text{Dec}_G)$ from a set of molecular hypergraphs (Section 5). In this section, we finally present an application of our encoders and decoders to molecular optimization, which aims to search a molecule with desirable properties.

6.1 Our Model

Our model consists of a pair of encoder and decoder, (Enc, Dec) , and a predictive model from the latent space to a target value. Our encoder and decoder are composed as:

$$\begin{aligned}\text{Enc} &= \text{Enc}_N \circ \text{Enc}_G \circ \text{Enc}_H, \\ \text{Dec} &= \text{Dec}_H \circ \text{Dec}_G \circ \text{Dec}_N,\end{aligned}$$

where $(\text{Enc}_N, \text{Dec}_N)$ is a seq2seq GVAE (Kusner et al., 2017). Since GVAE can output a parse sequence that follows a context-free grammar, Dec_N is guaranteed to output a valid parse sequence that belongs to $\text{Enc}_G[\mathcal{L}_{\text{MHG}}]$, the domain of the following decoder Dec_G .

Both Enc_N and Dec_N use three-layer GRU (Cho et al., 2014) with 384 hidden units (Enc_N is bidirectional), handling a sequence of production rule embeddings in 128-dimensional space. In Enc_N , the output of GRU is fed into a linear layer to compute the mean and log variance of a 72-dimensional Gaussian distribution, and the latent vector $z \in \mathbb{R}^{72}$ is sampled from it as the output of Enc_N . The encoder and decoder are trained by optimizing the objective function of β -VAE (Higgins et al., 2017) with $\beta = 0.01$ using ADAM (Kingma and Ba, 2015) with initial learning rate 5×10^{-4} . As a predictive model $\hat{f}: \mathbb{R}^{72} \rightarrow \mathbb{R}$, we employ a linear regression. Whenever target values are available, we jointly train seq2seq VAE and the predictive model.

Algorithm 1 summarizes our procedure to obtain latent representations of the input molecules. Note that this algorithm does not outputs encoders, because molecular optimization algorithms require Dec only.

6.2 Molecular Optimization Algorithms

We present two types of molecular optimization problem settings, as suggested by Jin et al. (2018).

Global molecular optimization (Problem 2) aims to find novel molecules with desirable properties from the whole molecular space. Algorithm 2 describes the procedure.

Local molecular optimization (Algorithm 3) aims to improve the property of a given molecule without modifying it too much. This problem setting is formalized as,

$$m^* = \text{Dec} \left(\arg \max_{z: \text{sim}(m, \text{Dec}(z)) \geq \tau} f(\text{Dec}(z)) \right). \quad (4)$$

where $\text{sim}(m, m')$ computes a similarity between molecules m and m' , and τ is a similarity threshold. We use Tanimoto similarity with Morgan fingerprint (radius=2). Problem 4 is approximately solved by Algorithm 3, where we substitute our predictive model \hat{f} for the unknown target function f .

7 Related Work

We introduce the existing literature of molecular optimization and discuss our contribution to this research area.

Molecular optimization has a longstanding history especially in drug discovery, and mostly combinatorial methods have been used to generate novel molecules (Jorgensen, 2009). The paper by Gómez-Bombarelli et al. (2018) gives rise to an alternative approach to this problem; they convert the combinatorial optimization problem into a continuous one with the help of

Algorithm 1 Latent Representation Inference

In: Mol. graphs and targets, $\mathcal{G}_0 = \{g_n\}_{n=1}^N$, $\mathcal{Y}_0 = \{y_n\}_{n=1}^N$.

- 1: Obtain molecular hypergraphs: $\mathcal{H}_0 \leftarrow \text{Enc}_H(\mathcal{G}_0)$
- 2: Obtain an MHG as well as parse sequences:
 $\text{Dec}_G, \text{MHG}, \mathcal{S}_0 \leftarrow \text{MHG-INF}(\mathcal{H}_0)$.
- 3: Train NNs using $(\mathcal{S}_0, \mathcal{Y}_0)$ to obtain $(\text{Enc}_N, \text{Dec}_N), \hat{f}$.
- 4: Obtain latent vectors, $\mathcal{Z}_0 \leftarrow \mathbb{E}[\text{Enc}_N[\mathcal{S}_0]]$.
- 5: **return** Latent vectors \mathcal{Z}_0 , Dec_G , Dec_N , \hat{f} .

Algorithm 2 Global Molecular Optimization

In: $\mathcal{Z}_0, \mathcal{Y}_0, \text{Dec}$, #iterations K , #candidates M .

- 1: $\mathcal{D}_1 \leftarrow \{(z_n, y_n)\}_{n=1}^N$
- 2: **for** $k = 1, \dots, K$ **do**
- 3: Fit a sparse GP using \mathcal{D}_k .
- 4: Obtain candidates $\mathcal{Z}_k = \{z_m \in \mathbb{R}^D\}_{m=1}^M$ from BO.
- 5: Obtain molecular graphs as $\mathcal{G}_k \leftarrow \text{Dec}[\mathcal{Z}_k]$.
- 6: Obtain target values as $\mathcal{Y}_k \leftarrow f[\mathcal{G}_k]$.
- 7: $\mathcal{D}_{k+1} \leftarrow \mathcal{D}_k \cup \{(z_{k,m}, y_{k,m}) \in \mathcal{Z}_k \times \mathcal{Y}_k\}_{m=1}^M$.
- 8: **return** Novel molecules $\{g_{k,m}\}_{m=1, k=1}^{M, K}$.

VAE. Since its earlier version appeared in 2016, a number of studies have been conducted to follow up this approach. As stated in the introduction, the decoding error issue has been one of the critical issues, and therefore, this section focuses on a series of studies alleviating it.

There are mainly two approaches to address this issue. One approach is to devise the decoding network to generate as valid SMILES strings as possible. For example, Kusner et al. (2017) leverages SMILES’ grammar to force the decoder to align the grammar. This approach is limited because they assume a context-free grammar (CFG), while SMILES’ grammar is not totally context-free. Dai et al. (2018) propose to use an attribute grammar, which enhances CFG by introducing attributes and rules. This enhancement allows us to enforce semantic constraints to the decoder. However, they deal only with the ring-bond matching and valence conditions, and therefore, their decoder sometimes fails to generate valid molecules.

Another approach is to substitute another molecular representation for SMILES so that the output is guaranteed to be valid. As far as we know, only the very recent paper by Jin et al. (2018) takes this approach. They represent a molecule by fragments connected in a tree structure. While their work for the first time reports 100% validity of decoded molecules, their method requires multiple neural networks other than VAE and the predictor. Our work further pushes along this direction by formalizing the tree representation in terms of HRG. This formalization allows us to model atom-level connections between fragments along with the stereochemistry information, and we realize 100% validity using a single VAE and the predictor.

8 Empirical Studies

We empirically evaluate the effectiveness of MHG in the molecular optimization domain. As baseline methods, we employ CVAE (Gómez-Bombarelli et al., 2018), GVAE (Kusner et al., 2017), SD-VAE (Dai et al., 2018), and JT-VAE (Jin et al., 2018). For their details, see Section 7. We basically follow Jin et al.’s experimental procedures, and the baseline results are copied from the paper. Table 1 summarizes our experimental results.

Dataset. We use the ZINC dataset following the existing work. This dataset is extracted from the ZINC database (Irwin et al., 2012) and contains 220,011 molecules for training, 24,445 for validation, and 5,000 for testing.

For the target chemical property to be maximized, we follow the existing work (Jin et al., 2018). In Section 8.2, we employ a standardized penalized logP:

$$f(m) = \widehat{\log P}(m) - \widehat{\text{SA}}(m) - \widehat{\text{cycle}}(m), \quad (5)$$

where $\log P$ is the octanol-water partition coefficient, SA is the synthetic accessibility score, and cycle is the number of rings whose length is longer than six, and the hat represents that the function is standardized using the values calculated on the

Algorithm 3 Local Molecular Optimization

In: Mol. graph g_0 and its latent vector z_0 , Dec, \hat{f} , step size η , similarity measure $\text{sim}(\cdot, \cdot)$, threshold τ , # iterations K .

```
1:  $g^* \leftarrow \text{null}, y^* \leftarrow -\infty$ 
2: for  $k = 1, \dots, K$  do
3:    $z_k \leftarrow z_{k-1} + \eta \frac{\partial \hat{f}(z_{k-1})}{\partial z}$ 
4:    $g_k \leftarrow \text{Dec}(z_k), y_k \leftarrow \hat{f}(z_k)$ 
5:   if  $\text{sim}(g_0, g_k) \geq \tau, g_0 \neq g_k$ , and  $y_k > y^*$  then
6:      $g^* \leftarrow g_k, y^* \leftarrow y_k$ 
7: return  $(g^*, y^*)$ 
```

Table 1: Experimental results.

Method	% Reconst.	% Valid prior	Log likelihood	RMSE	1st	2nd	3rd	50th	Top 50 Avg.
CVAE	44.6%	0.7%	-1.812 ± 0.004	1.504 ± 0.006	1.98	1.42	1.19	N/A	N/A
GVAE	53.7%	7.2%	-1.739 ± 0.004	1.404 ± 0.006	2.94	2.89	2.80	N/A	N/A
SD-VAE	76.2%	43.5%	-1.697 ± 0.015	1.366 ± 0.023	4.04	3.50	2.96	N/A	N/A
JT-VAE	76.7%	100%	-1.658 ± 0.023	1.290 ± 0.026	5.30	4.93	4.49	3.48	3.93
Ours	94.8%	100%	-1.323 ± 0.003	0.959 ± 0.002	5.56	5.40	5.34	4.12	4.49

δ	Improvement				Similarity				Success			
	0.0	0.2	0.4	0.6	0.0	0.2	0.4	0.6	0.0	0.2	0.4	0.6
JT-VAE	1.91 ± 2.04	1.68 ± 1.85	0.84 ± 1.45	0.21 ± 0.71	0.28 ± 0.15	0.33 ± 0.13	0.51 ± 0.10	0.69 ± 0.06	97.5%	97.1%	83.6%	46.4%
Ours	3.28 ± 2.19	2.40 ± 2.16	1.00 ± 1.87	0.61 ± 1.20	0.09 ± 0.06	0.26 ± 0.10	0.52 ± 0.11	0.70 ± 0.06	100%	86.3%	43.5%	17.0%

training set. For example, letting $\mu_{\log P}$ and $\sigma_{\log P}$ be the sample mean and standard deviation of $\log P$ calculated using the training set, $\widehat{\log P}(m) = (\log P(m) - \mu_{\log P}) / \sigma_{\log P}$. In Section 8.3, we use a penalized $\log P$:

$$f(m) = \log P(m) - \text{SA}(m). \quad (6)$$

8.1 Reconstruction Rate

Protocol. For each molecular graph m in the test set, we obtain its reconstruction as $m' = \text{Dec}(\text{Enc}(m))$. If m and m' are isomorphic, we regard the reconstruction succeeds. We repeat the above procedure using all of the test molecules 100 times, and report the mean reconstruction success rate.

To investigate the quality of the latent space, we evaluate the success rate of decoding random latent vectors. We sample z from $\mathcal{N}(0, I)$ and decode it to obtain $m = \text{Dec}(z)$. If m is valid, we regard the decode succeeds. We repeat this procedure 1,000 times and report the success rate.

Result. According to Table 1 (upper-left), our method clearly improves the reconstruction rate, which justifies our molecular modeling approach.

8.2 Global Molecular Optimization

Protocol. We first obtain latent representations by Algorithm 1. Then, we apply PCA to the latent vectors to obtain 40-dimensional latent representations. Then, we run Algorithm 2 with $M = 50$ and $K = 5$ to obtain 250 novel molecules. We repeat this procedure ten times, resulting in 2,500 novel molecules. We report (i) the log-likelihood and root mean-squared error (RMSE) of GP evaluated on the test set⁴, (ii) top three molecule property scores, and (iii) the mean of top 50 target

⁴Our method is evaluated on the held-out test set, whereas the existing ones use cross validation on the training set. While these scores measure the same predictive performance, our protocol is more reasonable, because VAE is trained on the whole training set.

properties.

Result. Table 1 (upper-mid) shows the predictive performance of GP. Our method achieves higher log-likelihood and lower RMSE, indicating that our latent space well encodes features necessary to predict the target property.

Table 1 (upper-right) reports the top three target properties as well as the minimum and average scores of top 50 molecules. Our top three molecules have the highest target properties. Furthermore, even if we focus on the statistics of top 50 molecules, our method achieves better scores than JT-VAE⁵. These results suggest that our method is more likely to discover better molecules. See Appendix C for the top 50 molecules we found.

8.3 Local Molecular Optimization

Protocol. We choose 800 molecules with the lowest penalized logP from the test set. For each initial molecule m , we run Algorithm 3 with $\tau \in \{0, 0.2, 0.4, 0.6\}$, $K = 80$, and $\eta = 0.01$. For each threshold τ , we report (i) the mean and standard deviation of the target value improvements, (ii) those of the similarity, and (iii) the success rate, where Algorithm 3 succeeds if the output is not null, *i.e.*, if there exists a modified molecule that satisfies the similarity constraint.

Result. Table 1 (lower) reports the scores. For any similarity threshold, our method improves the target property better than JT-VAE, which demonstrates the effectiveness of MHG-VAE. On the other hand, the success rate of our method is generally lower than that of JT-VAE, especially when the threshold is high. These results suggest that, if there are several candidate molecules, our method is favorable, because the outputs of our method will contain better improved molecules than JT-VAE; if a user wishes to improve the property of a specific molecule, JT-VAE can be favorable, because our method may not succeed to output a molecule that satisfies the similarity condition.

9 Conclusion and Future Work

We have developed the molecular hypergraph grammar variational autoencoder (MHG-VAE). Our key idea is to employ MHG to represent a molecular graph as a parse tree, which is fed into VAE. Since MHG models the atom-level connections as well as the stereochemistry information, MHG-VAE can learn a pair of encoder and decoder using a single VAE. The highlights of our experiments include (i) MHG-VAE can reconstruct molecules accurately, (ii) global optimization using MHG-VAE is more likely to find better molecules, and (iii) local optimization using MHG-VAE can improve the target property better than the existing methods.

A future research direction will be to optimize MHG with respect to some goodness criteria such as the minimum description length (Jonyer et al., 2004) or a Bayesian criterion (Chen, 1995). Since the resultant MHG depends on tree decompositions, we can optimize MHG by manipulating tree decompositions.

Another direction involves retrosynthetic analysis, which derives a pathway to synthesize the target molecule. With this capability, we will be able to immediately examine the property by synthesizing the output molecule.

Acknowledgments

This work was supported by JST CREST Grant Number JPMJCR1304, Japan, and JSPS KAKENHI Grant Numbers 15H05711, Japan. The author would like to thank Dr. Masakazu Ishihata for his helpful discussion.

References

Salvador Aguiñaga, Rodrigo Palacios, David Chiang, and Tim Weninger. Growing graphs from hyperedge replacement graph grammars. In *Proceedings of the 25th ACM International on Conference on Information and Knowledge Management (CIKM '16)*, pages 469–478, 2016.

⁵Since BO is a highly random procedure, examining only top three molecules could lead to unfair comparison, and we suggest to examine the statistics of top- K molecules.

- Stanley F. Chen. Bayesian grammar induction for language modeling. In *Proceedings of the 33rd Annual Meeting on Association for Computational Linguistics*, ACL '95, pages 228–235, Stroudsburg, PA, USA, 1995. Association for Computational Linguistics. doi: 10.3115/981658.981689. URL <https://doi.org/10.3115/981658.981689>.
- Kyunghyun Cho, Bart van Merriënboer, Caglar Gulcehre, Dzmitry Bahdanau, Fethi Bougares, Holger Schwenk, and Yoshua Bengio. Learning phrase representations using RNN encoder–decoder for statistical machine translation. In *Proceedings of the 2014 Conference on Empirical Methods in Natural Language Processing*, pages 1724–1734, 2014.
- Hanjun Dai, Yingtao Tian, Bo Dai, Steven Skiena, and Le Song. Syntax-directed variational autoencoder for structured data. In *International Conference on Learning Representations*, 2018.
- Frank Drewes, H-J. Kreowski, and Annegret Habel. *Hyperedge replacement graph grammars*, volume 1, chapter 2, pages 95–162. 1997.
- Rafael Gómez-Bombarelli, Jorge Aguilera-Iparraguirre, Timothy D. Hirzel, David Duvenaud, Dougal Maclaurin, Martin A. Blood-Forsythe, Hyun Sik Chae, Markus Einzinger, Dong-Gwang Ha, Tony Wu, Georgios Markopoulos, Soonok Jeon, Hosuk Kang, Hiroshi Miyazaki, Masaki Numata, Sunghan Kim, Wenliang Huang, Seong Ik Hong, Marc Baldo, Ryan P. Adams, and Alan Aspuru-Guzik. Design of efficient molecular organic light-emitting diodes by a high-throughput virtual screening and experimental approach. *Nat Mater*, 15(10):1120–1127, 10 2016. URL <http://dx.doi.org/10.1038/nmat4717>.
- Rafael Gómez-Bombarelli, Jennifer N. Wei, David Duvenaud, José Miguel Hernández-Lobato, Benjamín Sánchez-Lengeling, Dennis Sheberla, Jorge Aguilera-Iparraguirre, Timothy D. Hirzel, Ryan P. Adams, and Alán Aspuru-Guzik. Automatic chemical design using a data-driven continuous representation of molecules. *ACS Central Science*, 01 2018. doi: 10.1021/acscentsci.7b00572. URL <https://doi.org/10.1021/acscentsci.7b00572>.
- Irina Higgins, Loic Matthey, Arka Pal, Christopher Burgess, Xavier Glorot, Matthew Botvinick, Shakir Mohamed, and Alexander Lerchner. β -VAE: Learning basic visual concepts with a constrained variational framework. In *Proceedings of 2017 International Conference on Learning Representations*, 2017.
- John J. Irwin, Teague Sterling, Michael M. Mysinger, Erin S. Bolstad, and Ryan G. Coleman. ZINC: A free tool to discover chemistry for biology. *Journal of Chemical Information and Modeling*, 52(7):1757–1768, 2012.
- Wengong Jin, Regina Barzilay, and Tommi Jaakkola. Junction tree variational autoencoder for molecular graph generation. In *Proceedings of the Thirty-fifth International Conference on Machine Learning (ICML-18)*, 2018.
- Istvan Jonyer, Lawrence B. Holder, and Diane J. Cook. MDL-based context-free graph grammar induction and applications. *International Journal on Artificial Intelligence Tools*, 13(1):65–79, 2004.
- William L Jorgensen. Efficient drug lead discovery and optimization. *Accounts of chemical research*, 42(6):724–733, 06 2009. doi: 10.1021/ar800236t. URL <http://www.ncbi.nlm.nih.gov/pmc/articles/PMC2727934/>.
- Diederik Kingma and Jimmy Ba. Adam: A method for stochastic optimization. In *Proceedings of the Third International Conference for Learning Representations*, 2015.
- Diederik P. Kingma and Max Welling. Auto-encoding variational bayes. In *Proceedings of the International Conference on Learning Representations*, 2014.
- Matt J. Kusner, Brooks Paige, and José Miguel Hernández-Lobato. Grammar variational autoencoder. In *Proceedings of the 35th International Conference on Machine Learning*, 2017.
- J. Močkus. On Bayesian methods for seeking the extremum. In G. I. Marchuk, editor, *Optimization Techniques IFIP Technical Conference Novosibirsk, July 1–7, 1974*, pages 400–404, Berlin, Heidelberg, 1975. Springer Berlin Heidelberg. ISBN 978-3-540-37497-8.
- David Weininger. SMILES, a chemical language and information system. 1. introduction to methodology and encoding rules. *Journal of Chemical Information and Computer Sciences*, 28(1):31–36, 02 1988. doi: 10.1021/ci00057a005. URL <https://pubs.acs.org/doi/abs/10.1021/ci00057a005>.

Algorithm 4 Production rule extraction

Input: tree decomposition T and node $v_T \in V_T$.

Output: production rule $p = (A, R)$.

- 1: Find $\text{pa}(v_T)$ and $\text{ch}(v_T)$.
 - 2: **if** $\text{pa}(v_T)$ does not exist **then**
 - 3: Set A as the starting hyperedge S .
 - 4: **else**
 - 5: Set $A = \ell_T^{(V)}(v_T) \cap \ell_T^{(V)}(\text{pa}(v_T))$.
 - 6: Set $R = H(v_T)$, where the nodes shared with A are set to be the external nodes, $\text{ext}(R)$.
 - 7: **if** $\text{ch}(v_T)$ is not empty **then**
 - 8: **for** each child $v'_T \in \text{ch}(v_T)$ **do**
 - 9: Add a non-terminal hyperedge to R , which consists of nodes $\ell_T^{(V)}(v_T) \cap \ell_T^{(V)}(v'_T)$ with the non-terminal label.
 - 10: **return** (A, R)
-

A HRG Inference Algorithm

This section describes the details of the algorithm proposed by Aguiñaga et al..

The input of the algorithm is a set of hypergraphs, $\hat{\mathcal{H}} = \{H_1, \dots, H_N\}$, and its output is a hyperedge replacement grammar \mathcal{G} whose language includes the input hypergraphs. The algorithm extracts production rules from each input hypergraph. Let $H \in \hat{\mathcal{H}}$ be any input hypergraph. It first computes a tree decomposition of H , which we denote by T , and picks an arbitrary node of T as its root. Then, for each node $v_T \in V_T$, it applies Algorithm 4 to extract a production rule. Algorithm 4 chooses the triplet of v_T and its parent and children as shown in Figure 5a, and extracts a production rule that glues $H(v_T)$ to $H(\text{pa}(v_T))$ with non-terminal hyperedges for gluing each child. Figure 5b illustrates the production rule extracted from the triplet shown in Figure 5a. After applying Algorithm 4 to all of the nodes and all of the input hypergraphs, it removes duplicated production rules and outputs the set of production rules.

B Proofs

This section provides a proof of Theorem 2. Throughout this section, a *node* refers to a hypergraph's node, and a *tree node* refers to a tree decomposition's node.

To prove Theorem 2, we only have to prove that $\mathcal{L}_{\text{HRG}}(\hat{\mathcal{H}}) \subseteq \mathcal{H}(L_H^{(V)}, L_H^{(E)}, c^{(E)})$ holds, because $\hat{\mathcal{H}} \subseteq \mathcal{L}_{\text{HRG}}(\hat{\mathcal{H}})$ has been proven by Aguiñaga et al..

$\mathcal{L}_{\text{HRG}}(\hat{\mathcal{H}}) \subseteq \mathcal{H}(L_H^{(V)}, L_H^{(E)}, c^{(E)})$ can be proven by combining Lemmata 4, 5, and 6. Lemmata 4 and 5 guarantee that our algorithm preserves the first condition of a molecular hypergraph, and Lemma 6 guarantees that our algorithm preserves the second condition of a molecular hypergraph.

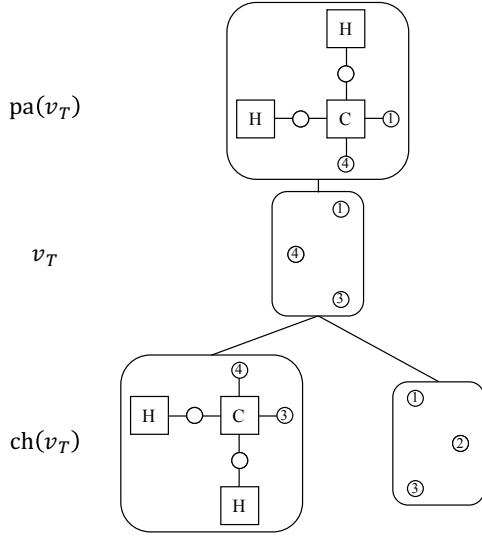
Condition 3. For each production rule $p = (A, R)$, the degree of external nodes of R is one, and the degree of internal nodes of R is two.

Lemma 4. HRG inferred by applying our algorithm to a set of 2-regular hypergraphs satisfies Condition 3.

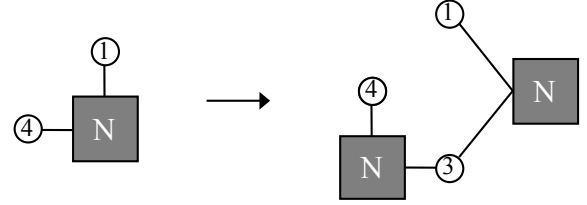
Lemma 5. If HRG satisfies Condition 3, then it always generates a 2-regular hypergraph.

Lemma 6. HRG inferred by applying our algorithm to a set of cardinality-consistent hypergraphs always generates a cardinality-consistent hypergraph.

Proof of Lemma 4. Let H be an arbitrary input hypergraph, and $(T, \ell_T^{(V)}, \ell_T^{(E)})$ be its irredundant tree decomposition. Since H is 2-regular, for each $v_H \in V_H$, $T[V_T(v_H)]$ is a single tree node that contains both of the two hyperedges (Figure 6a, **Case 1**), or $T[V_T(v_H)]$ is a path where each of the leaf tree nodes contains one of two hyperedges adjacent to v_H (Figure 6b, **Cases 2, 3**). It is sufficient to prove that for each $v_H \in V_H$ and for each $v_T \in T[V_T(v_H)]$, the production rule extracted by running Algorithm 4 satisfies Condition 3. In the following, we fix $v_H \in V_H$ to be an arbitrary node and $e_{H,1}, e_{H,2} \in E_H$ to be the hyperedges incident with v_H .

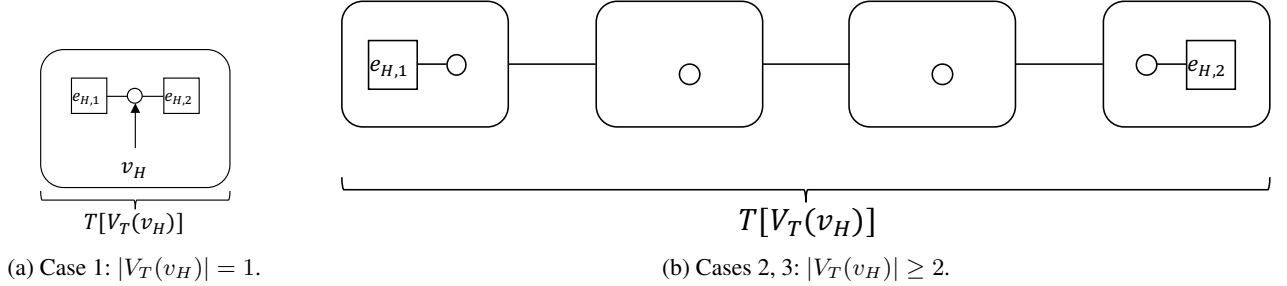


(a) Triplet of v_T , $\text{pa}(v_T)$, and $\text{ch}(v_T)$ chosen from the tree decomposition in Figure 3.



(b) Production rule extracted from the triplet in Figure 5a. Nodes IDs are added for explanation, and in the algorithm, they are removed except for the correspondence between the nodes in LHS and the external nodes in RHS.

Figure 5: Illustration of Algorithm 4.



(a) Case 1: $|V_T(v_H)| = 1$.

(b) Cases 2, 3: $|V_T(v_H)| \geq 2$.

Figure 6: Illustrations of $T[V_T(v_H)]$ in two cases.

Case 1. $|V_T(v_H)| = 1$

First, let us assume $|V_T(v_H)| = 1$ and let v_T^* be the only node in $V_T(v_H)$, i.e., $V_T(v_H) = \{v_T^*\}$. In this case, v_H cannot be an external node, because $\text{pa}(v_T^*)$ does not contain v_H . Thus, v_H must be an internal node with $e_{H,1}$ and $e_{H,2}$ when it appears in R . In addition, no non-terminal hyperedge will be incident with v_H in R , because none of $\text{ch}(v_T^*)$ contains v_H in it. Therefore, in this case, v_H is an internal node whose degree equals two in R .

Case 2. $|V_T(v_H)| \geq 2$ and v_H is an internal node in R

Such a production rule is made from a triplet $(v_T, \text{pa}(v_T), \text{ch}(v_T))$ such that $v_H \in \ell_T^{(V)}(v_T)$ and $v_H \notin \ell_T^{(V)}(\text{pa}(v_T))$ hold.

If $e_{H,1} \in \ell_T^{(E)}(v_T)$ or $e_{H,2} \in \ell_T^{(E)}(v_T)$ holds, there exists exactly one node $v_T^{(\text{ch})} \in \text{ch}(v_T)$ such that $v_H \in \ell_T^{(V)}(v_T^{(\text{ch})})$ holds. In this case, exactly one non-terminal hyperedge will be connected to v_H , and therefore, the degree of v_H equals two in R .

If $e_{H,1} \notin \ell_T^{(E)}(v_T)$ and $e_{H,2} \notin \ell_T^{(E)}(v_T)$ hold, there exist exactly two nodes $v_{T,1}^{(\text{ch})}, v_{T,2}^{(\text{ch})} \in \text{ch}(v_T)$ such that $v_H \in \ell_T^{(V)}(v_{T,1}^{(\text{ch})})$ and $v_H \in \ell_T^{(V)}(v_{T,2}^{(\text{ch})})$ hold. In this case, exactly two non-terminal hyperedges will be connected to v_H , and therefore, the degree of v_H equals two in R .

Case 3. $|V_T(v_H)| \geq 2$ and v_H is an external node in R

Such a production rule is made from a triplet $(v_T, \text{pa}(v_T), \text{ch}(v_T))$ such that $v_H \in \ell_T^{(V)}(v_T)$ and $v_H \in \ell_T^{(V)}(\text{pa}(v_T))$ hold.

If $e_{H,1} \in \ell_T^{(E)}(v_T)$ or $e_{H,2} \in \ell_T^{(E)}(v_T)$ holds, for each node $v_T^{(\text{ch})} \in \text{ch}(v_T)$, $v_H \notin \ell_T^{(V)}(v_T^{(\text{ch})})$ holds. In this case, no non-terminal hyperedge will be connected to v_H , and therefore, the degree of v_H equals one in R .

If $e_{H,1} \notin \ell_T^{(E)}(v_T)$ and $e_{H,2} \notin \ell_T^{(E)}(v_T)$ hold, there exists exactly one node $v_T^{(\text{ch})} \in \text{ch}(v_T)$ such that $v_H \in \ell_T^{(V)}(v_T^{(\text{ch})})$ holds. In this case, exactly one non-terminal hyperedge will be connected to v_H , and therefore, the degree of v_H equals one in R .

Therefore, for any case, Condition 3 holds, and therefore, Lemma 4 has been proven. \square

Proof of Lemma 5. Let H be an arbitrary hypergraph that can be derived from the starting symbol S . Note that H may contain non-terminal hyperedges. It is sufficient to prove that H is 2-regular, if the production rules satisfy Condition 3.

If H is directly derivable from the starting symbol S , then it is 2-regular, because Condition 3 guarantees that for any production rule $p = (S, R)$, R is 2-regular.

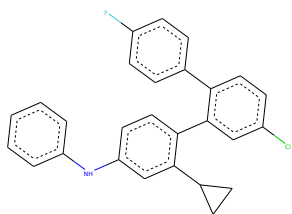
If H is directly derivable from H' by applying $p = (A, R)$, and if H' is 2-regular and derivable from S , then there exists a non-terminal hyperedge in $e_{H'} \in E_{H'}$ that is labeled as A and is replaced with R to yield H . For each node $v_{H'} \in V_{H'} \setminus e_{H'}$, the replacement does not change the degree, and the degree of $v_{H'}$ equals two in H . For each node $v_R \in V_R \setminus \text{ext}(R)$ ⁶, the replacement does not change the degree, and the degree of v_R equals two in H . For each node $v_{H'} \in e_{H'}$, the replacement first deletes $e_{H'}$, and then, connects the hyperedges adjacent to the external nodes $\text{ext}(R)$. Since the degrees of the external nodes are one, the replacement does not change its degree. The same applies to each external node. Since the degree of each node of H is two, H is proven to be 2-regular. \square

Proof of Lemma 6. Let T be a tree decomposition of a molecular hypergraph H . For each $v_T \in V_T$, all of the hyperedges in $\ell_T^{(E)}(v_T)$ are cardinally-consistent, which is guaranteed by the second condition in Definition 1. Therefore, letting the production rule extracted from v_T be $p = (A, R)$, all of the hyperedges in R are cardinally-consistent. Since applying such a production rule preserves the cardinality consistency, this lemma has been proven. \square

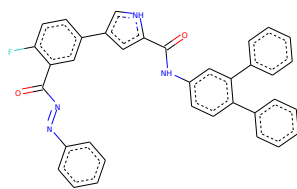
C Molecules Discovered by Global Molecular Optimization

In the following, we illustrate the top 50 molecules found by global molecular optimization in Section 8.2.

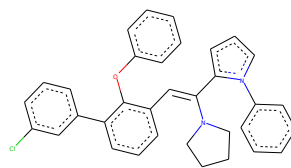
⁶ $\text{ext}(R)$ denotes the set of external nodes in R



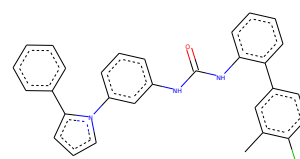
5.558



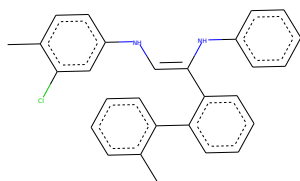
5.401



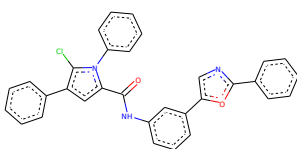
5.344



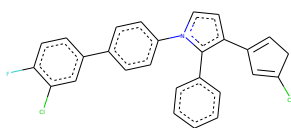
5.289



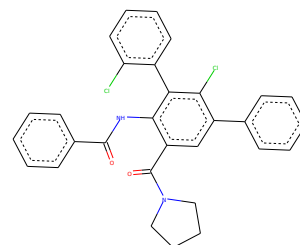
5.063



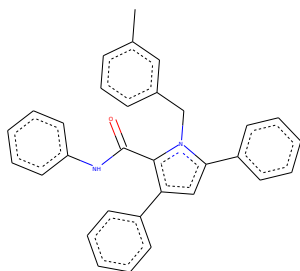
4.979



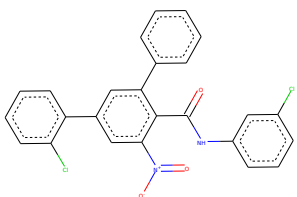
4.811



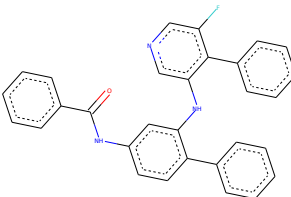
4.779



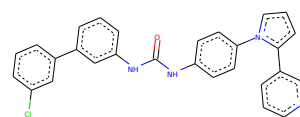
4.775



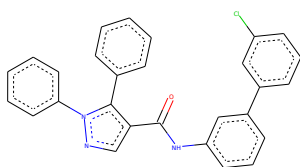
4.730



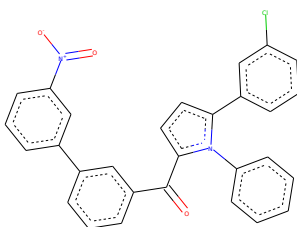
4.712



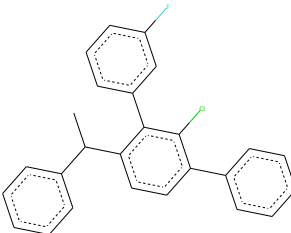
4.641



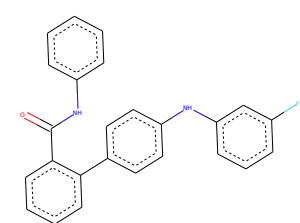
4.617



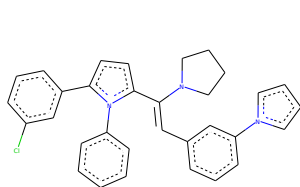
4.598



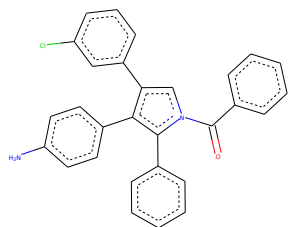
4.595



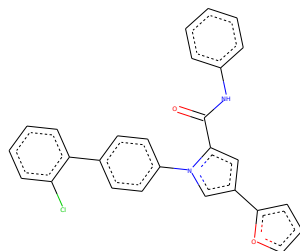
4.555



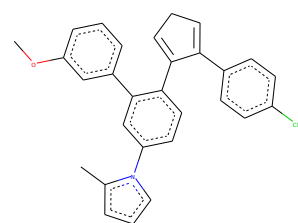
4.546



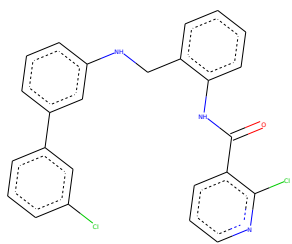
4.538



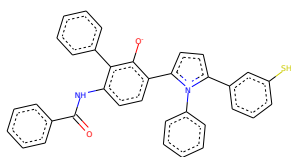
4.484



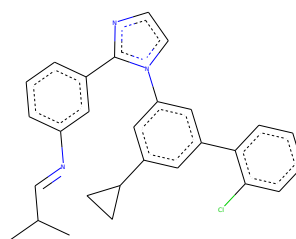
4.464



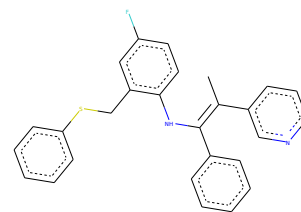
4.450



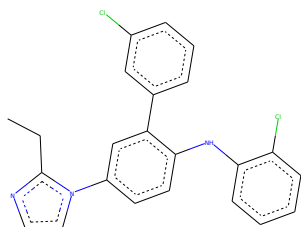
4.443



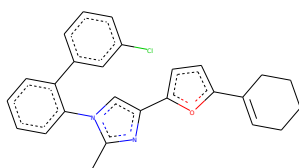
4.408



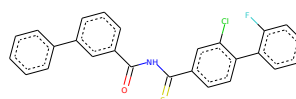
4.404



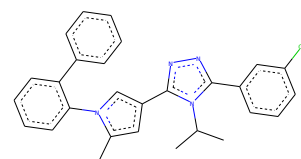
4.374



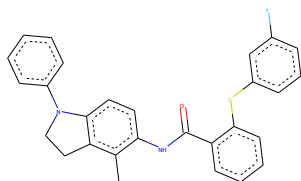
4.362



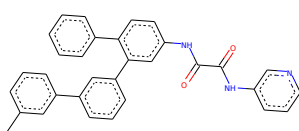
4.354



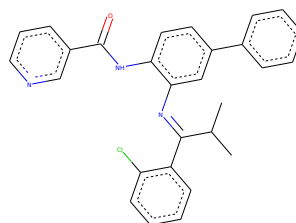
4.351



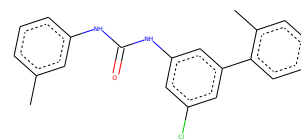
4.349



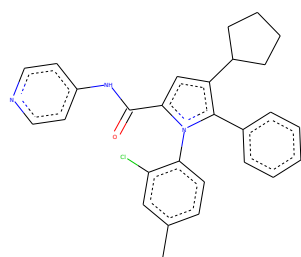
4.341



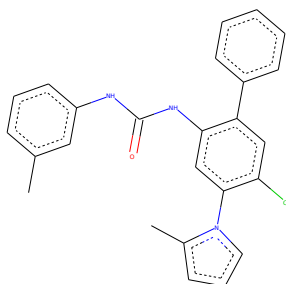
4.335



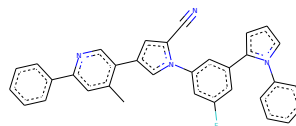
4.294



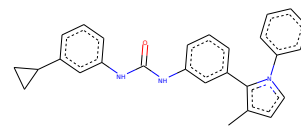
4.274



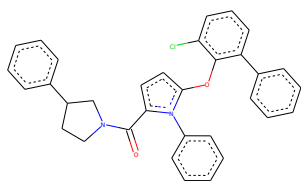
4.265



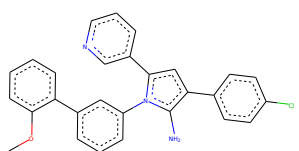
4.259



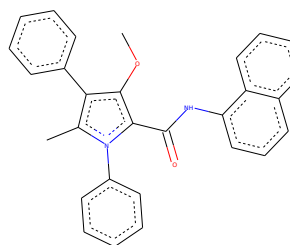
4.258



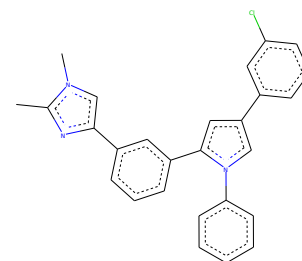
4.242



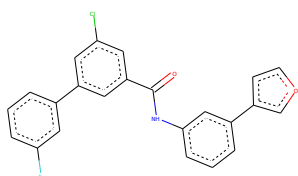
4.240



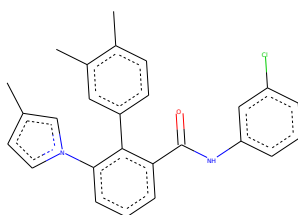
4.233



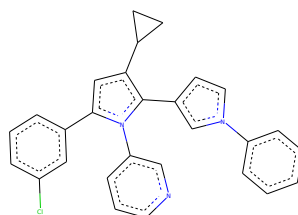
4.209



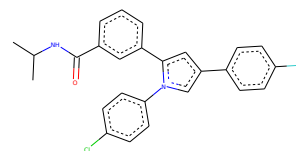
4.202



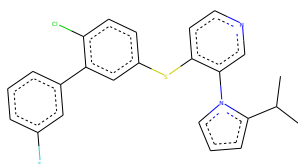
4.196



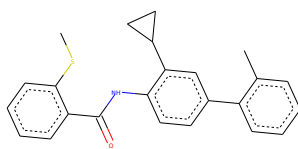
4.185



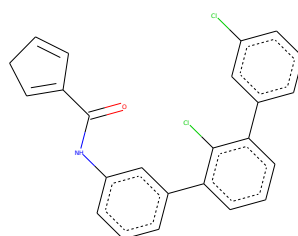
4.171



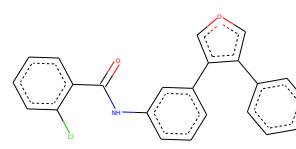
4.169



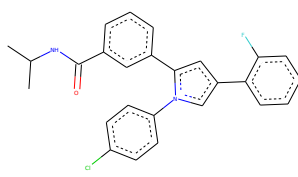
4.163



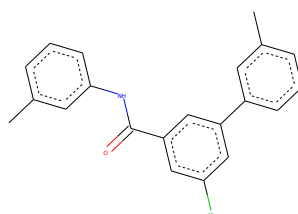
4.153



4.150



4.124



4.124